ORIGINAL ARTICLE

A C G publications

Rec. Nat. Prod. X:X (202X) XX-XX

records of natural products

Discriminating Metabolites of *Curcuma caesia* and *Kaempferia parviflora* through ^{1}H-NMR and GC-MS Analysis for Plant Authentication

Muhammad Safwan Ahamad Bustamam [1], Siok-Geok Chong [1], Wei-Ming Heng [2], M. Akmal M. Nazri [2], Emelia Asmara Md Daud [2], Nur Aqilah Lakowi [2] Mohd Saipullah Mohd Daud [3], Geoffrey A. Cordell [4] and Intan Safinar Ismail [1,2*]

[1] *Natural Medicines and Products Research Laboratory, Institute of Bioscience, Universiti Putra Malaysia, 43400 UPM Serdang, Selangor Darul Ehsan, Malaysia*

[2] *Department of Chemistry, Faculty of Science, Universiti Putra Malaysia, 43400 UPM Serdang, Selangor Darul Ehsan, Malaysia*

[3] *Berkat Curcuma Caesia Sdn. Bhd., No. 9 Dataran Kg.Sri Jaya, 81900 Kota Tinggi, Johor Darul Takzim, Malaysia*

[4] *Natural Products Inc., Evanston, IL 60201, USA; Department of Pharmaceutics, College of Pharmacy, University of Florida, Gainesville, FL 32610, USA*

(Received September 13, 2024; Revised November 18, 2024; Accepted November 22, 2024)

Abstract: The current study aimed to characterize the metabolite fingerprints of the rhizomes of *Curcuma caesia* Roxb. (KH) and *Kaempferia parviflora* Wall. ex Baker (HH) in the family Zingiberaceae using a combination of ^{1}H-NMR and GC-MS analyses. There are authentication issues between these two species, wherein both are commonly commercialized as Kunyit Hitam (KH) or Black Turmeric, the local name only for *C. caesia*. *K. parviflora* is locally known as Halia Hitam (HH) or Black Ginger. The metabolite profile for each species was analyzed through 1H-NMR data by multivariate data analysis (MVDA) to determine the chemical markers. Orthogonal Partial Least Square-Discriminant Analysis (OPLS-DA) showed clusters of the two species in which the Variable Importance in Projection (VIP) values of more than 1 yielded eleven and four discriminated metabolites belonging to *C. caesia* (KH) and *K. parviflora* (HH) respectively. The hexane extracts of the rhizomes of KH and HH were subjected to GC-MS profiling which resulted in 22 and 24 metabolites, respectively and terpenoids, flavonoids, and alkanes were tentatively identified in KH and HH. This study developed characteristic metabolite fingerprinting profiles for each species which distinguish between the rhizomes unambiguously and provide an authenticity assessment of the available products for the patient's benefit.

Keywords: *Curcuma caesia; Kaempferia parviflora;* NMR spectroscopy; multivariate analysis; authentication; marker compounds.

* Corresponding author: E-Mail: safinar@upm.edu.my ; Phone: +603-97697492 *Fax:+603-97693237*

The article was published by ACG Publications
http://www.acgpubs.org/journal/records-of-natural-products Month-Month 202x EISSN:1307-6167
DOI: http://doi.org/10.25135/rnp.488.2409.3327
Available online: January 01, 2025

1. Introduction

Curcuma caesia Roxb., also referred to commercially as Black Turmeric or Black Zedoary and locally known as Kunyit Hitam (KH), is a lesser-known species in the Zingiberaceae. It is a perennial plant characterized by its distinctive purplish-bluish-black-ringed rhizome possessing a bitter and pungent camphorous odor [1]. The plant originates from India, where it is commonly known as Kali Haldi in Hindi, and it thrives in moist deciduous forest areas in the northeast regions of Arunachal Pradesh and Manipur. The rhizome is traditionally utilized to treat sprains, bruises, migraine, snake or scorpion bites, bloating and stomach ache, and is also used by tribal women as a facial mask for their engagement and wedding preparations [2]. It is extensively cultivated as a medicinal plant in various southeast Asian countries, including Indonesia, Thailand, and Malaysia, due to its wide range of reported pharmacological activities, including antioxidant, antimicrobial, anticancer, anti-inflammatory, antidepressant, antidiabetic, analgesic, and thrombolytic effects [3–12].

Kaempferia parviflora, known as Halia Hitam (HH) or Black Ginger, is a Zingiberaceae species originating from Thailand, and is popularly recognized as Krachaidum or Thai ginseng. This medicinal plant has now spread widely across some local tropical regions, including Malaysia, Sumatra, and Borneo Island. Its dark purplish rhizome has a long history of use as a traditional medicine. Biological studies on extracts of the rhizome have revealed anti-allergic, anti-inflammatory, antimutagenic, antidepressant, anticholinesterase, antimicrobial, anticancer, anti-peptic ulcer, cardioprotective, anti-obesity, and aphrodisiac effects [13].

Recently, there was a surge in the popularity of KH products, particularly in the forms of instant "coffee" and capsules in Malaysia. The hype of possessing a diverse range of medicinal benefits has enhanced the panacea-like marketing of the plant products. However, based on unpublished studies from this laboratory, many of the commercialized products claiming to contain KH are not derived from authentic *C. caesia* (KH). It appears to be commonly found, intentionally or not, that there is a confusion regarding the identification of the two species, *Curcuma caesia* and *Kaempferia parviflora*.

The identification and authentication of medicinal plant products are of increasing and significant global concern, particularly in countries such as China, India, Japan, Korea, United States and many other countries where alternative and complementary medicines play a prominent role in primary healthcare [14–16]. The World Health Organization (WHO), the United States Food and Drug Administration (USFDA), and the European Medicines Agency (EMEA) have emphasized that validated primary assays are necessary to ensure the initial authentication of plant-based medicines and to distinguish them from related species or to identify adulterated traditional medicines [17,18]. Such an establishment of authenticity does not however, indicate either safety or effectiveness with respect to health benefit claims.

The growing awareness and global societal concerns related to plant-based medicinal products, including their adulteration, authenticity, safety, effectiveness, and consistency have prompted scientists to develop complex DNA-based and chemically-based analytical methods for the authentication and analysis of plant mixtures to demonstrate the variability in their chemical compositions and thus their likely biological outcomes [18–20]. Comprehensive chemical profiling has become an essential analytical tool, serving as a specific signature for a particular part of a plant, which, in many instances, enables the analytical method to be used for initial quality control purposes [21]. Methods for assuring biological consistency in medicinal plant products remain to be developed.

Metabolite fingerprinting refers to the detailed analysis of the constituents in a specific extract of single or mixed, plant-based medicines. Subsequent data processing through chemometric techniques may then facilitate characterization, differentiation, and classification of their origins [22]. High-field Nuclear Magnetic Resonance (NMR) spectroscopy offers several advantages for analysing and authenticating medicinal plant extracts due to its rapidity, simplified sample preparation, high reproducibility, and robustness. NMR can also simultaneously analyse primary and secondary metabolites comprehensively in a specific sample [23, 24]. When combined with multivariate analysis chemometrics, such as principal component analysis (PCA), partial least square-discriminant analysis (PLS-DA), and OPLS-DA, which can effectively rationalize the substantial data sets generated, NMR becomes an effective tool for the metabolite

fingerprinting of medicinal plants [25, 26]. Numerous recent studies have applied this analytical approach, including for the classification of three *Curcuma* species, the discrimination of black pepper samples based on their geographical origins, and the authentication and standardization of Tongkat Ali.(*Eurycoma longifolia*) [27–29]. However, a single analytical process of an extract cannot provide a complete metabolite profile and identification within a specific plant sample. This is due to the differing volatilities, polarities, and complexities of the metabolite composition when extractive solvents of different polarities are used. Combination with other separation techniques and spectroscopic tools provides greater analytical depth, and enhanced sensitivity and reliability of the overall metabolite profile. Gas chromatography coupled with mass spectrometry (GC-MS) is a rapid and sensitive technique for the identification of volatile and semi-volatile compounds in medicinal plant extracts. Many phytochemicals, such as terpenoids, aldehydes, ketones, alcohols, esters, flavonoids, and phenolics, from Zingiberaceae species have been successfully identified by GC-MS [30–32]. Thus, combining the two analytical tools of NMR and GC-MS for the metabolite fingerprinting of KH and HH was anticipated to address the authentication issue between the rhizomes of these species. Additionally, establishing a more detailed and robust metabolite profile of KH might serve in developing a quality control standard for robust authentication as an ingredient in products claiming to contain KH.

2. Materials and Methods

2.1. Plant Collection, Authentication, and Extract Preparations

Rhizomes of *Curcuma caesia* Roxb. (KH) and *Kaempferia parviflora* Wall. ex Baker (HH) were cultivated in the same plot (GPS: 1º40’42.6”N 103º49’38.9”E) in Kota Tinggi, Johor by Berkat Curcuma Caesia Sdn. Bhd. (BCC) and harvested after 3 months as six replicates of each species. Authentication of the plant samples was performed through the complementary methods of the inspection of plant morphology and DNA marker analysis. The two species were identified morphologically by an in-house botanist, Dr. Mohd Firdaus Ismail, Biodiversity Unit, Institute of Bioscience, Universiti Putra Malaysia (UPM), and the voucher specimens of KH (MFI 0219/21) and HH (KM 0029/22) were deposited in the herbarium of the Biodiversity Unit, Institute of Bioscience, Universiti Putra Malaysia (UPM). The DNA barcoding of the rhizomes was conducted at the Forest Research Institute Malaysia (FRIM) following their Standard Operating Procedure using internal transcribed spacer 2 (ITS2) regions of nuclear ribosomal DNA (nrDNA) sequences. Subsequently, the DNA sequences were subjected to BLAST analysis against FRIM’s DNA barcoding database (MyBARCODE). Phylogenetic inference was also performed using Neighbor-joining (NJ) analysis [33]. The rhizomes were prepared for chemical analysis by washing in water, patting with tissue paper, and oven drying (ProTech, Balakong, Selangor, Malaysia) at 60ºC for 24 hrs [34]. After drying, the rhizomes were ground to a powder in the range 1.54-4.17 g and then stored at -20ºC until analysed.

2.2. 1D- and 2D-NMR Measurements

A sample (50 mg) of each rhizome powder was directly extracted through sonication for 20 min at room temperature with CD_3OD:D_2O (1:1) containing 0.05% trimethylsilyl propanoic acid (TSP) as an internal reference standard for NMR analysis. After sonication, the mixture was centrifuged at 13,000 rpm (11,200 x *g*-force) for 10 min. A sample (600 µL) of the supernatant was transferred to a 5 mm NMR tube and analyzed on a 500 MHz Varian Unity INOVA NMR spectrometer (Varian Inc., Palo Alto, CA, USA) operating at a frequency of 499.91 MHz and maintained at 26°C. For data acquisition, a single-pulse proton experiment with presaturation (PRESAT) was used with 21.0 µsec pulse width, 2-sec relaxation delay, and a 3.53 min total acquisition time for 64 scans. A two-dimensional *J*-resolved experiment (JRES) was used to assist in clarifying the spectral assignments. The *J*-resolved spectrum was acquired over 50 min and 18 s, with 8 scans per 256 increments for the axis of the spin-spin coupling constant and spectral widths of 66

Hz, and 8 K data points for the chemical shift axis with spectral widths of 8012.8 Hz. The relaxation delay was set at 1.0 s. Heteronuclear single quantum coherence (HSQC) spectra were obtained using 16 scans, 1 K data points, and 256 increments at the spectral width of 13 and 220 ppm for the proton (^{1}H) and carbon (^{13}C) dimensions, respectively. The relaxation delay was 1.0 s, giving an achievement time of 369 min and 9 s. The 2D-NMR spectral processing for structural elucidation was carried out using MestRenova software (Version 6.02-5475, Mestrelab Research, Santiago de Compostella, Spain).

2.3. NMR Data Processing

Phasing and baseline corrections of NMR spectra were carried out using Chenomx software (Version 5.1, Edmonton, AL, Canada) and referenced to the internal standard (TSP) at 0.00 ppm. The ^{1}H-NMR spectrum of each sample was processed and bucketed or binned in the width of 0.04 ppm within the spectral region 0.30 to 10.00 ppm. The peaks for residual water (4.80–4.90 ppm) and methanol (3.30-3.32 ppm) were excluded from the spectral data to retain the signals from the endogenous metabolites. A total of 239 integrated bins were obtained for each spectrum. The generated datasets were converted to XLSX files and used for multivariate data analysis.

2.4. Multivariate data analysis

The processed spectroscopic data were analyzed using multivariate data analysis of Principal Component Analysis (PCA) and Orthogonal Partial Least Square-Discriminant Analysis (OPLS-DA) models using SIMCA-P 14.1 software (Umetrics, Umeå, Sweden). The dataset was Pareto-scaled, and a score plot was constructed to visualize the separation between groups, while a loading plot was used to identify those metabolites that contributed to their separation. The model was validated using the default seven-fold internal cross-validation based on the goodness-of-fit (R2X) and goodness-of-prediction (Q2) values, together with the 100-permutation test [35].

2.5. Gas Chromatography-Mass Spectrometry (GCMS) Analysis

Individual samples (200 mg each) of the dried and ground KH and HH rhizomes were extracted with hexane (1.5 mL). The extracts were sonicated for 15 min at room temp before centrifugation for 10 min at 5,000 rpm (1,600× *g*-force). This step was repeated three times to obtain a pooled extract (4.5 mL) and was followed by overnight air-drying under a fume-hood at room temp. Each extract was dissolved in GCMS-grade hexane at 30,000 ppm and sonicated until dissolved.

The hexane extracts of each rhizome were analyzed using a Shimadzu GCMS-QP2010 Ultra system operating at 70 eV ionization energy. A Rxi-5MS (RESTEK) fused-silica-capillary column (30 m length; 0.25 mm ID; 0.25 μm film thickness) was used to separate the compounds. Helium was used as carrier gas in the split mode of ratio 1:10 with parameters set at pressure: 37.1 kPa; total flow: 11.8 mL/min; column flow: 0.80 mL/min; linear velocity: 32.4 cm/sec; and purge flow: 3.0 mL/min. The column temperature was programmed from 50 to 300°C at a rate of 3°C/min and a hold for 10 min. The injector and ion source temperatures were 250 and 200°C, respectively. Identification of the detected compounds was accomplished based on a comparison of their mass spectra and retention times with the available in-house spectral libraries including NIST11, NIST17, Flavour and Fragrance Natural and Synthetic Compounds (FFNSC) Version 1.3, and Wiley 229. Percent peak areas (%) were calculated by dividing the area response for a particular peak by the total responses from all detected peaks.

2.6. Statistical Analysis

Significant differences between the samples were evaluated using the independent sample *t*-test with a confidence interval of 95% ($p < 0.05$).

3. Results and Discussion

3.1 Plant Species Authentication

For species verification, there are several important morphological characteristics that are typically observed for plants. Figure 1a shows the intact KH plant attached with large oblong, lanceolate. glabrous leaves. The lamina in the central section of leaf has rich ferruginous purple clouds. The primary roots are not visible when the plant propagates through the rhizome; nevertheless, golden brown, long fibrous and tapered adventitious roots are present all over the surface of the rhizome. The rhizome is tuberous with a camphorous, fragrant odor, and is 2-6 cm in diameter, with a varying form and size. It has longitudinal circular wrinkles on the surface with a distinguishing bluish-black color [36]. Meanwhile, *K. parviflora* (HH) is a low-growing plant with tuberous roots. The leaves are ovate, erect, or apprised to the soil with a yellow-green color also at the margin site, as depicted in Fig. 1b. Compared with KH, the internal color of the HH rhizome is dark purple to black [37].

(a) (b)

Figure 1. Morphological comparison of whole plant and rhizome of (a) *C. caesia* (KH) and (b) *K. parviflora* (HH)

Despite several morphological characteristics, including leaf shape, and leaf and rhizome color and the KH camphoraceous smell, which do differentiate the two species, molecular characterization or DNA markers enhance the authentication and support the morphological evaluation, particularly when the aerial parts are not available. Therefore, the internal transcribed spacer (ITS) regions of nuclear ribosomal DNA (nrDNA) sequences from the two rhizomes were examined. The DNA sequences of ITS2 for 010B23 (KH) and 012B23 (HH) are presented in Supporting Information 1. The BLAST results of ITS2 showed 100% similarity between 010B23 and *C. caesia* (Fig. 2a). Similarly, the ITS2-based Neighbor-joining (NJ) analysis revealed that 010B23 was clustered under a well-supported clade with *C. caesia* (Fig. 2c; highlighted in red). Meanwhile, the BLAST results of ITS2 indicated 100% similarity between 012B23 and

K. parviflora (Fig. 2b). The ITS2-based NJ analysis also revealed that 012B23 was clustered under a well-supported clade with *K. parviflora* (Fig. 2c; highlighted in blue). Based on these DNA findings, 010B23 (KH) was authenticated as *C. caesia* and 012B23 (HH) as *K. parviflora*.

Query ID	Subject ID	% identity	Alignment length	Mismatches	Evalue	Bit score
010B23	011B23	100.000	167	0	2.74E-85	302
010B23 & 011B23	*Curcuma caesia*	100.000	179	0	5.85E-92	324
010B23 & 011B23	*Curcuma aeruginosa*	97.765	179	4	1.27E-88	313
010B23 & 011B23	*Curcuma longa*	95.876	97	4	4.85E-43	161
010B23 & 011B23	*Zingiber zerumbet*	89.286	112	12	6.32E-37	141
010B23 & 011B23	*Zingiber montanum*	83.246	191	20	2.90E-45	169
010B23 & 011B23	*Kaempferia pulchra*	83.051	177	22	6.28E-42	158
010B23 & 011B23	*Kaempferia parviflora*	80.645	155	30	2.29E-31	122

(a)

Query ID	Subject ID	% identity	Alignment length	Mismatches	Evalue	Bit score
012B23	013B23	100.000	169	0	1.19E-88	313
012B23 & 013B23	*Kaempferia parviflora*	100.000	169	0	1.19E-88	313
012B23 & 013B23	*Zingiber zerumbet*	91.538	130	8	1.63E-47	176
012B23 & 013B23	*Zingiber montanum*	89.231	130	10	1.64E-42	159
012B23 & 013B23	*Kaempferia pulchra*	88.372	172	9	3.47E-54	198
012B23 & 013B23	*Kaempferia galanga*	86.441	177	11	3.50E-49	182
012B23 & 013B23	*Curcuma aeruginosa*	78.986	138	29	1.01E-24	100
012B23 & 013B23	*Curcuma caesia*	78.986	138	29	1.30E-23	97.1

(b)

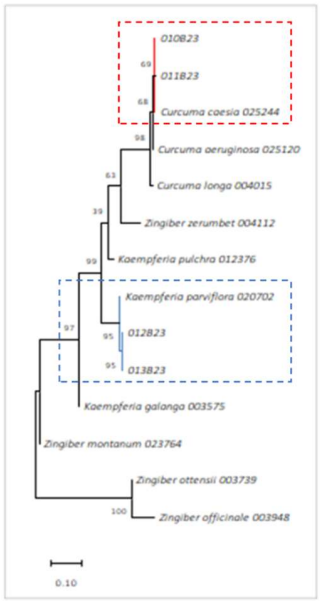

(c)

Figure 2. BLAST results for the ITS2 regions of (a) *C. caesia*, KH; (b) *K. parviflora*, HH; and (c) the Neighbor-joining analysis on the sequences of ITS2 region with bootstrap values generated from 1,000 replications

3.2. Metabolite Identification Using 1D- and 2D-NMR

Analysis of the 1D- and 2D-^{1}H-NMR spectra of a specific extract may be used to assist in the authentication of an acquired medicinal plant as they offer a fingerprint based on well-defined, specific spectral patterns of the constituent metabolites [27]. Figure 3 shows the representative ^{1}H-NMR spectra corresponding to KH and HH. For improved spectral interpretation, the data are divided into three main regions for aliphatic (0.20–3.00 ppm), carbohydrate (3.01–5.00 ppm), and aromatic (6.00–9.00 ppm) protons. Identification of the peaks was achieved by referring to previous studies on the same plant species and the exploration of freely available online databases such as the Human Metabolome Database (HMDB), with a focus on natural metabolites. Confirmation of the structural assignments was aided by information from 2D *J*-resolved and ^{1}H-^{13}C HSQC correlation data, as provided in Table 1 and Supporting Information 2. Initial visual inspection reveals that the KH and HH extracts exhibit quite different NMR spectral patterns in each region of their metabolite matrices.

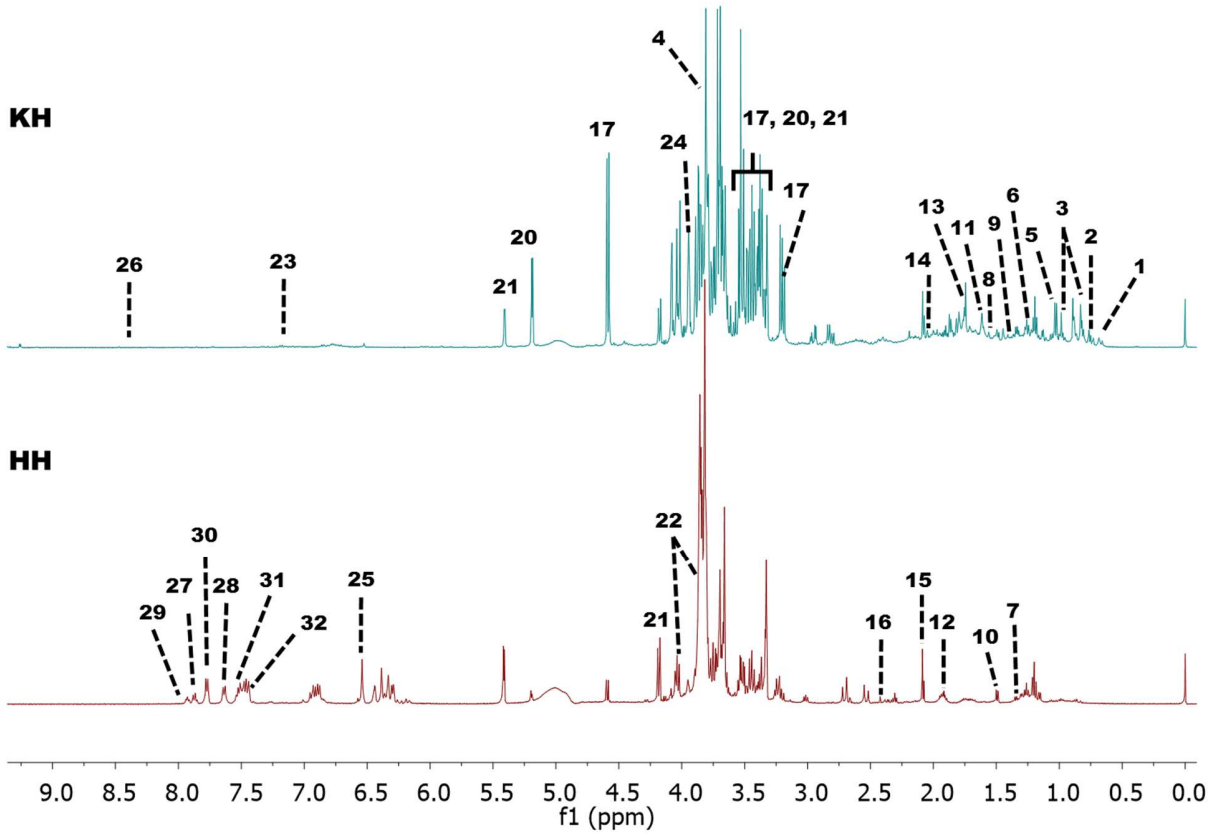

Figure 3. Representative 500 MHz ^{1}H-NMR spectra of KH and HH in CD_3OD:D_2O (1:1) containing 0.05% TSP with assignments of the peaks as listed in Table 1

Twenty-five metabolites from different chemical classes were tentatively identified in the CD_3OD:D_2O (1:1) extract of KH rhizome material (Table 1). The aliphatic region of KH was mostly considered to be due to terpenoids and some amino acids (Figure 3). The identifications of the metabolites were made based on the previously reported studies of *C. caesia* and other *Curcuma* species [38], [41]. The presence of camphor was indicated by three, 3H singlets at 0.83, 0.89, and 0.98 ppm attributable to the methyl groups which, in HSQC, showed correlations with C-1, C-6, and C-8 at 21.85, 11.33, and 21.20 ppm, respectively [39]. A bicyclic monoterpenoid, 1,8-cineole or eucalyptol, was assigned based on the singlet methyl signal at 1.22 ppm with HSQC correlations to C-9/10 at 34.25 ppm [44]. Another terpenoid detected in the KH rhizome was the sesquiterpenoid germacrone, and was confirmed through the correlation of three, 3H singlets at δ_H 1.61, 1.74, and 1.81 which correlated in the HSQC spectrum with the carbons at δ_C 18.53, 23.31, and 24.40, respectively [41]. The presence of zedoalactone A was confirmed through the correlation of a methine singlet at δ_H 5.91 with the carbon resonance at δ_C 95.49. Identification of zerumin B was verified by a singlet methylene resonance at δ_H 4.08 (-CH_2) directly correlated to its carbon at δ_C 85.58 in the 10-membered ring [45].

Table 1. Characteristic ^{1}H-NMR resonances of metabolites identified in the KH and HH rhizome extracts in $CD_3OD:D_2O$ (1:1)

No.	Tentative Metabolite Assignment	δ_H (ppm), multiplicity, *J* (Hz)	HSQC (^{1}H-^{13}C)	KH	HH	Ref.
1.	Zerumin B	0.68 (s)	16.94	+	-	[38]
		2.42 (s)	37.07			
		4.08 (s)	85.58			
2.	Amadaldehyde	0.76 (d, *J* = 6.3)	16.66	+	-	[38]
		0.86 (d, *J* = 2.4)	-			
3.	Camphor	0.83 (s)	21.85	+	-	[39]
		0.89 (s)	11.33			
		0.98 (s)	21.20			
4.	Amadannulen	0.82 (s)	23.85	+	-	[40]
		0.88 (s)	35.79			
		3.80 (s),	84.23			
5.	Valine	1.03 (d, *J* = 6.9)	21.36	+	-	[38]
		1.13 (d, *J* = 4.8)	20.93			
6.	1,8-Cineole/ Eucalyptol	1.22 (s)	34.52	+	-	[41]
7.	Threonine	1.35 (d, *J* = 9.8)	23.20	+	+	[38]
		3.48 (d, *J* = 9.8)	75.01			
8.	Zedoalactone A	1.35 (s)	-	+	-	[41]
		1.56 (s)	18.52			
		5.91 (s)	95.49			
9.	Camphene	1.45 (s)	17.76	+	-	
10.	Alanine	1.49 (d, *J* = 7.3)	15.88	+	+	[41]
11.	Germacrone	1.61 (s)	18.53	+	-	[41]
		1.74 (s)	23.31			
		1.81 (s)	24.40			
		2.94 (d, *J* = 4.0)	-			
		3.40 (d, *J* = 2.0)	80.04			
12.	Leucine	1.70 (m),	41.66	+	+	[41]
		3.70 (m)	64.14			
13.	Zedoalactone B	1.75 (s)	23.31	+	-	[41]
		1.90 (s)	25.14			
		6.02 (s)	-			
		6.07 (s)	-			
14.	*β*-Turmerone	1.80 (s)	24.42	+	-	[41]
		2.05 (s)	25.68			
15.	Methionine	2.09 (s)	-	+	+	[41]
		3.87 (m)	64.00			
16.	Succinate	2.41 (s)	37.07	-	+	[42]
17.	*β*-Glucose	3.20 (dd, *J* = 7.9, 9.2)	78.49	+	+	[38]
		3.36 (dd, *J* = 3.9, 9.6)	73.11			
		4.58 (d, *J* = 7.9)	99.46			
18.	Choline	3.22(s)	56.92	+	+	[38]
19.	Betaine	3.28 (s)	-	+	-	[42]
		3.89 (d, *J* = 1.9)	64.11			

20.	*α*-Glucose	3.36 (dd, *J* = 3.9, 9.6)	73.11	+	+	[38]
		3.47 (dd, *J* = 3.7, 9.8)	75.32			
		3.68 (t, *J* = 4.5)	67.08			
		5.19 (d, *J* = 3.7)	95.69			
21.	Sucrose	3.43 (t, *J* = 4.0)	79.44	+	+	[38]
		3.51 (dd, *J* = 4.1, 5.8)	67.60			
		3.65 (s)	65.57			
		3.74 (d, *J* = 4.1)	64.52			
		4.03 (d, *J* = 8.5)	77.64			
		4.17 (d, *J* = 8.7)	80.48			
		5.41 (d, *J* = 3.8)	95.46			
22.	*α*-Fructose	3.86 (dd, *J* = 2.0, 3.9)	64.52	+	+	[27]
		4.08 (d, *J* = 5.8)	78.92			
23.	Curcumin	3.92 (s)	-	+	-	[41]
		6.80 (d, *J* = 7.7)	115.67			
		7.19 (d, *J* = 8.0)	-			
		7.28 (s)	-			
24.	*β*-Fructose	3.94 (m)	72.62	+	+	[27]
25.	Fumaric acid	6.54 (s)	108.85	+	+	[27]
26.	Formic acid	8.48 (s)	-	+	-	[38]
27.	5,7,4′-Trimethoxyflavone	3.86 (s)	81.48	-	+	[43]
		6.38 (d, *J* = 1.9)	92.48			
		6.56 (s)	-			
		7.78 (d, *J* = 9.9)	129.30			
28.	3,7-Dimethoxy-5-hydoxyflavone	3.83 (s)	55.31	-	+	[43]
		3.85 (s)	72.41			
		6.38 (d, *J* = 1.9)	92.48			
		7.48 (m)	128.47			
29.	5,7-Dimethoxyflavone	3.96 (s)	69.28	-	+	[43]
		6.38 (d, *J* = 1.9)	92.48			
		7.48 (m)	128.47			
		7.88 (t, *J* = 8.3)	127.61			
30.	5-Hydroxy-3,7,3′,4′-tetramethoxyflavone	3.85 (s)	72.41	-	+	[43]
		3.86 (s)	81.48			
		3.96 (s)	69.28			
		6.38 (d, *J* = 1.9)	92.48			
		7.70 (d, *J* = 7.6)	125.44			
31.	3, 5, 7, 4′-Tetramethoxyflavone	3.76 (s)	72.60	-	+	[43]
		3.82 (s)	62.07			
		3.99 (s)	-			
		6.16 (d, *J* = 8.9)	95.54			
		6.89 (d, *J* =8.9)	113.62			
32.	5,7,3′,4′-Tetramethoxyflavone	3.93 (s)	-	-	+	[43]
		3.96 (s)	69.28			
		3.97 (s)	-			
		3.99 (s)	-			
		6.39 (d, *J* = 1.9)	106.52			
		7.38 (d, *J* = 1.5)	110.05			

Multiplicity assignments: s-singlet; d-doublet; t-triplet; dd-doublet of doublets; m-multiplet; *J*-coupling constant in Hz.Positive (+) and negative (-) signs denote the presence or absence of a metabolite, respectively.

Metabolites of *Curcuma caesia* and *Kaempferia parviflora*

Eighteen metabolites were tentatively identified in the CD_3OD:D_2O (1:1) extract of the HH rhizome material. As summarized in Table 1, and in contrast with the KH extract, most of the metabolites were carbohydrates and flavonoids. The downfield region from δ_H 6.00 to 8.00 displayed signals for the aromatic resonances of the flavonoids, along with a few additional signals in the aliphatic region (0.8-2.5 ppm). These observations allowed the preliminary identification of several methoxyflavone derivatives. However, significant complications were encountered due to the small differences caused by the number of methoxy groups (-OCH_3) and their respective locations on the flavone scaffold [43]. Confirmation of the methoxyflavone derivatives was aided by ^{1}H-^{13}C HSQC correlations, as displayed in Fig. 4. The presence of 5,7,4′-trimethoxyflavone **(1)** is supported by a methine doublet (-CH) at δ_H 7.81 correlated with C-2′ at δ_C 129.30. Meanwhile a methine doublet resonance at δ_H 7.70 correlated with the carbon at δ_C 125.44 suggested the presence of 5-hydroxy-3,7,3’,4’-tetramethoxyflavone **(2)**. The identification of 3,5,7,4’-tetramethoxyflavone **(3)** was justified through the correlation of a doublet methine resonance at δ_H 6.89 with C-3′/C-5′ at δ_C 113.62. The correlation of a methine proton presenting as triplet at δ_H 7.88 with the carbon at δ_C 127.61 suggested the presence of 5,7-dimethoxyflavone **(4)**. Furthermore, the presence of 5,7,3’,4’-tetramethoxyflavone **(5)** was justified by the correlation of a doublet methine resonance at δ_H 7.38 attached to δ_C 110.05 [46].

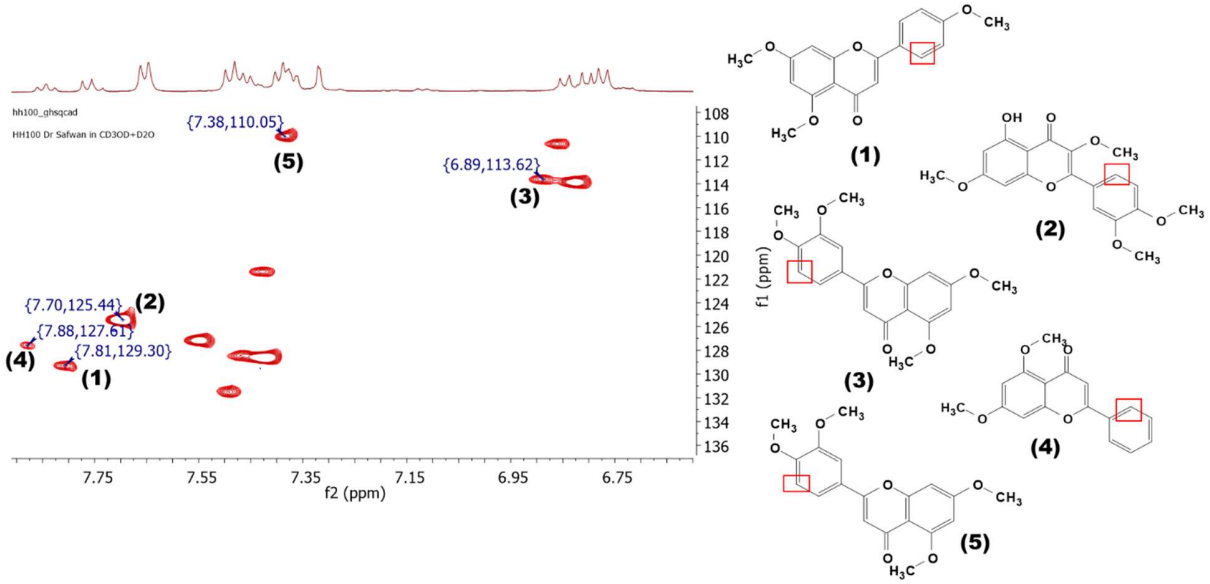

Figure 4. 2D-HSQC spectra of the HH extract in the downfield region for the identification of various methoxyflavone derivatives. The resonances are assigned as follows: **(1)** 5,7,4′-Trimethoxyflavone; **(2)** 5-Hydroxy-3,7,3’,4’-tetramethoxyflavone; **(3)** 3,5,7,4’-Tetramethoxyflavone; **(4)** 5,7-Dimethoxyflavone; and **(5)** 5,7,3’,4’- Tetramethoxyflavone

3.3. ^{1}H-NMR Metabolite Fingerprinting Through Multivariate Data Analysis

Multivariate data analysis (MVDA) was applied to determine the chemical variation between the samples of KH and HH rhizomes (n=6/each). The ^{1}H-NMR datasets for KH and HH were subjected to unsupervised principal component analysis (PCA) as a primary overview for any possible outliers. The PCA model obtained consisted of five principal components with excellent goodness (R^2X) and high predictability (Q2) values of 0.980 and 0.931, respectively (Supporting Information 3a). The PCA score plot (Supporting Information 3b) shows that the KH and HH rhizome samples are discriminated in different regions with 69% of the variance in the first principal component (PC1), while the second principal component (PC2) gave 19%, with a cumulative variance of 88%. The presence of potential outliers was

investigated by distance to the model (DModX) and Hotelling's T2 plot. There was only one insignificant outlier among the KH samples identified in DModX plots as depicted in Supporting Information 3c. However, the value was not twice as large as the maximum tolerable distance (Dcrit) and could be considered as only a moderate outlier. This was confirmed by Hottelling's T2 plot (Supporting Information 3d) which showed no strong outlier observed with all values within the 95% confidence limit. Hence, all the variables were retained for the subsequent statistical analysis.

Further classification was performed using the OPLS-DA model to discriminate the two groups observed in the PCA model and to generate information on the discriminating metabolites among the groups [47]. This technique is a supervised method, requiring class label information in building the appropriate model for data interpretation. Two components were generated with excellent fit and predictability as presented by values of R2Y = 0.998 and Q2Y= 0.995 (Fig. 5a). The validation of the supervised statistical approach, such as PLS or OPLS-DA, is critical due to the risk of the over-fitting model. A hundred random permutations test was conducted for each group (Fig. 5b) and achieved excellent validity after the R2 and Q2 intercepts did not exceed 0.3–0.4 and 0.05, respectively [35]. Another validation tool that was considered is the CV-ANOVA value which was below 0.05 indicating that this model is not over-fitted [48].

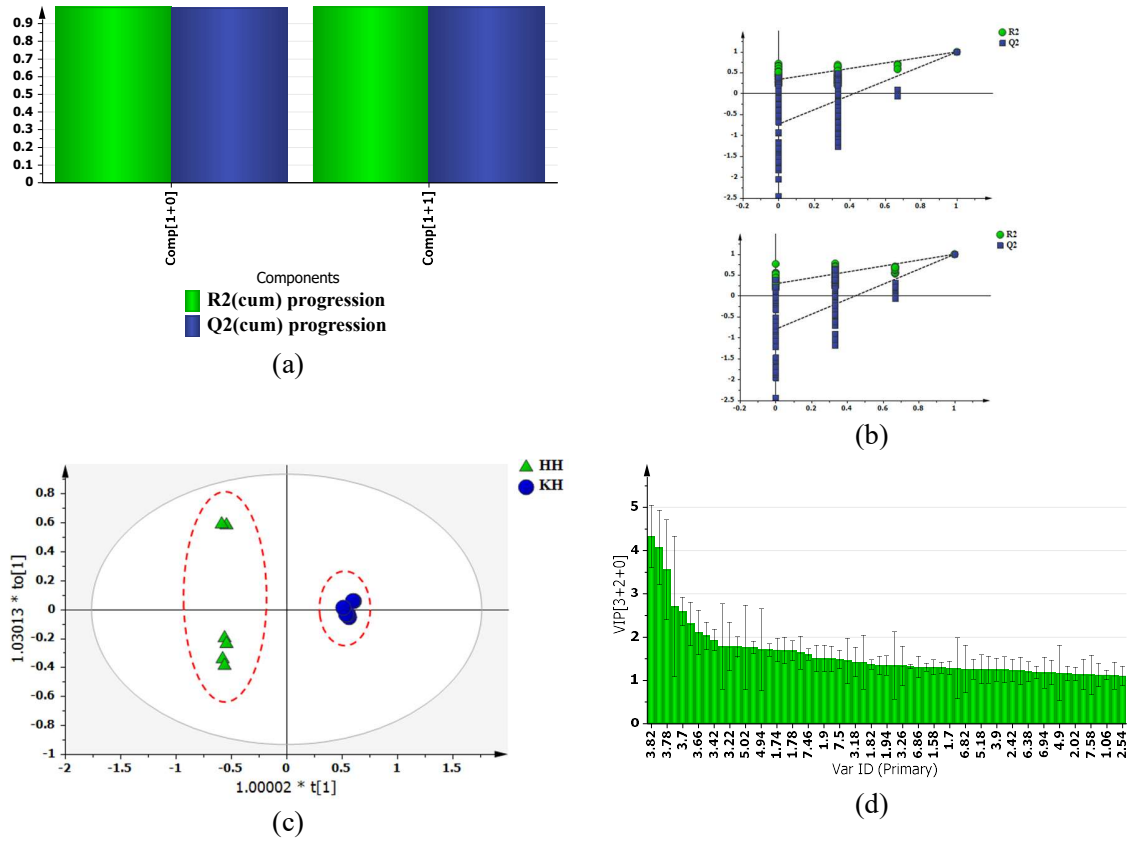

Figure 5. OPLS-DA model generated between the extracts of the KH and HH rhizomes; (a) summary of fit, (b) permutation test, (c) score plot, and (d) VIP plot

The OPLS-DA score plot (Fig. 5c) shows that the KH and HH extracts were discriminated by PC1. The importance and significance of the metabolites that are responsible for the separation for each plant were determined by analyzing the Variable Importance in Projection (VIP) plot with jack-knifing uncertainty bars as shown in Fig. 5d. The variables with VIP scores greater than 1 with an error bar not crossing the baseline in the loading column plot were retained as significant and were classified as chemical markers that gave an influential contribution to the discrimination in the OPLS model [49]. Based on their VIP values greater than 1.0, a total of 54 binned regions were selected as potential chemical markers that significantly contributed to the class separation as depicted in Fig. 5d. However, only 15 of these were identified with clear peaks observed as single metabolites without overlapping with other peaks. Their significance was evaluated using the *t*-test (with $p < 0.05$) and could be observed in box plots (Fig. 6) calculated using the web-based software MetaboAnalyst 5.0.

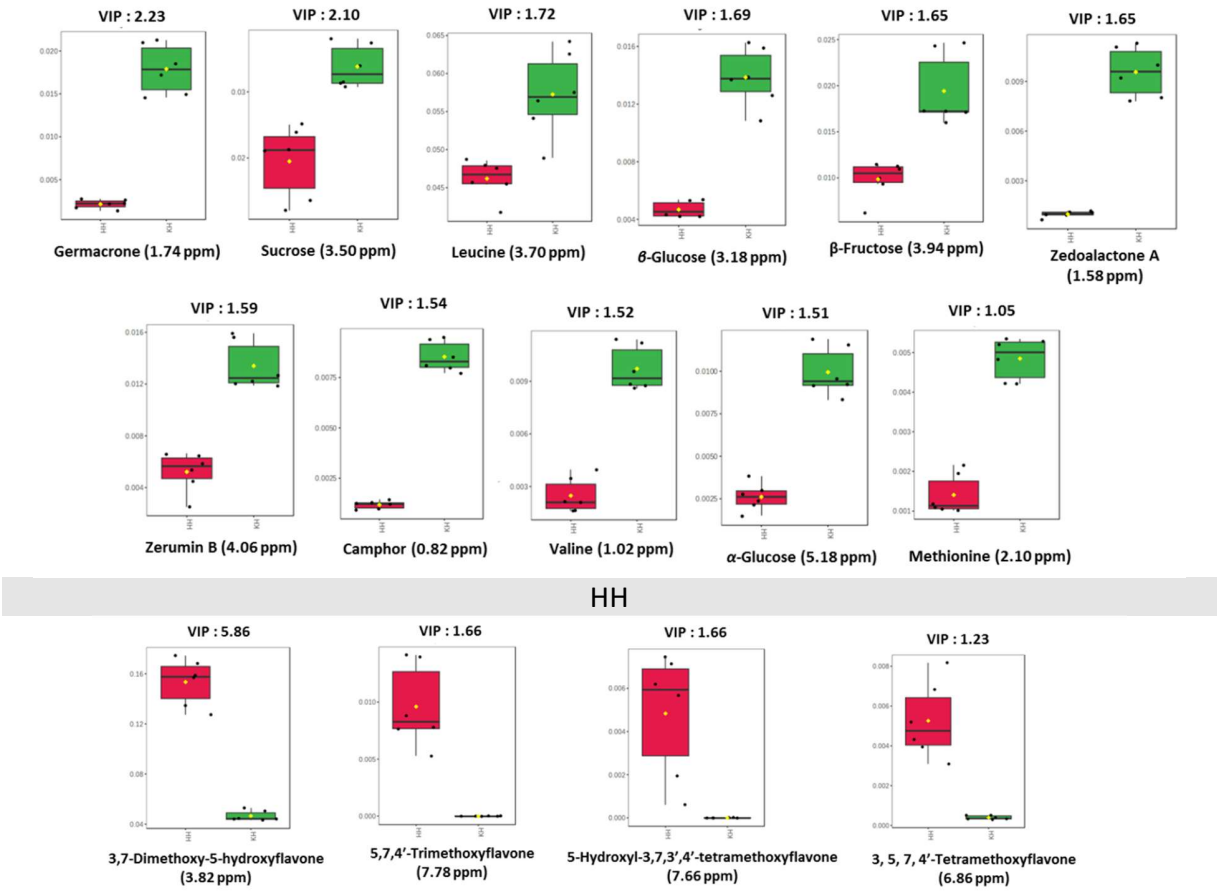

Figure 6. The box plot of potential chemical markers for the KH and HH extracts derived from the OPLS-DA model based on VIP > 1.0. The significance between them ($p<0.05$) was calculated based on the mean peak area of the ^{1}H-NMR resonances determined by the independent t-test

Based on the box plots in Fig. 6, there are 11 metabolites that can be assigned as chemical markers for KH, and are represented in green as germacrone, sucrose, leucine, *β*-glucose, α-glucose, zedoalactone A, *β*-fructose, zerumin B, camphor, valine, amadaldehyde, and methionine. These metabolites were present at a higher level ($p < 0.05$) in KH compared to HH, with camphor being one of the main bioactive metabolites present in *C. caesia* (KH) [50]. Four flavonoids could be assigned as markers for *Kaempferia parviflora* (HH) with significant intensities ($p < 0.05$) represented in red in Fig. 6. Numerous studies have

successfully determined the flavonoid composition of HH in different locations, as summarized in a recent review of *Kaempferia* species[51].

3.4 Metabolite Identification by GC-MS

Identification of the metabolites in the hexane extracts of KH and HH was achieved through GC-MS analysis. The total ion chromatograms (TIC) in Fig. 7 show the peaks detected in the KH and HH hexane extracts. Details of the tentative identifications of the metabolites are presented in Table 2 with a high similarity index score (more than 70%) based on the comparison of the obtained spectra with those in the National Institute of Standards and Technology (NIST) 08 and Flavour and Fragrance Natural and Synthetic Compounds (FFNSC) databases. The retention indexes (RI) were determined using Kováts' method, with alkane series ranging from C7 to C33. Forty-five metabolites were annotated from both plant species comprising several chemical classes, mainly terpenoids, flavonoids, alkanes, steroids, and esters.

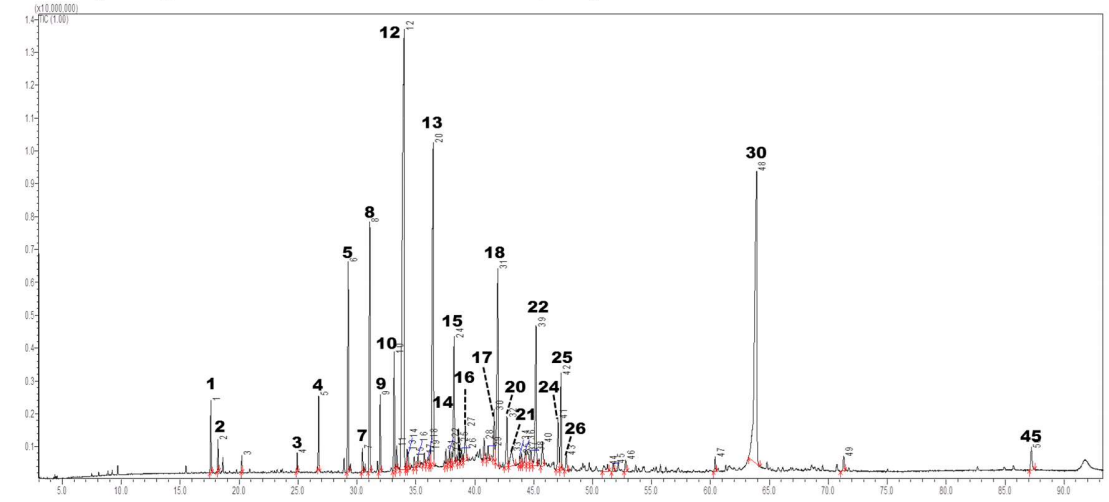

(a)

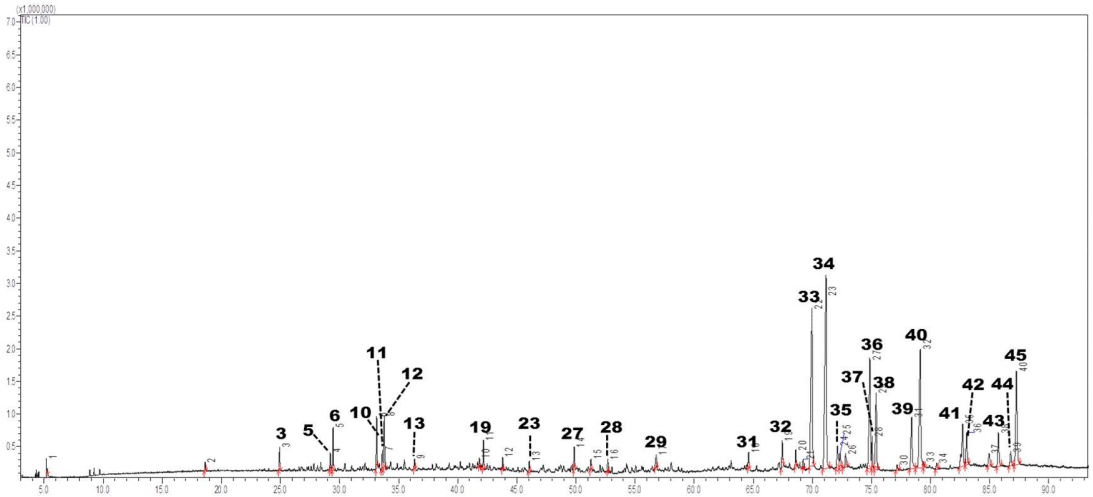

(b)

Figure 7. Total ion chromatogram (TIC)-GC-MS of a) KH hexane extract and b) HH hexane extract. The assignment of the peaks as listed in Table 2

Table 2. Tentative identification of metabolites in the KH and HH hexane extracts by GC-MS with relative intensity (%). Positive (+) and negative (-) signs denote presence and absence, respectively

Peak no.	RT (min)	Tentative Compound	Molecular Weight	Main class	Molecular fragments (*m/z*)	Similarity Index (SI)	Retention Index (RI)	KH (%)	HH (%)
1.	17.60	Camphor	152	Terpenoid	41, 55, 69, 81, 95, 108, 152	97	1144	+ (1.24)	-
2.	18.20	Isoborneol	154	Terpenoid	27, 41, 53, 77, 95, 110, 136	96	1157	+ (0.50)	-
3.	24.93	Tridecane	184	Alkane	41, 43, 57, 71, 85, 97, 127	96,95	1299	+ (0.29)	+ (0.83)
4.	26.77	*δ*-Elemene	204	Terpenoid	41, 51, 77, 93, 105, 121, 136	98, 97	1340	+ (1.28)	-
5.	29.26	*β*-Elemene	204	Terpenoid	41, 53, 67, 77, 81, 105, 107	98, 95	1395	+ (4.24)	+ (0.70)
6.	29.46	Tetradecane	198	Alkane	43, 57, 71, 85, 99, 127, 155	96	1400	-	+ (1.64)
7.	30.47	Caryophyllene	204	Terpenoid	41, 55, 69, 91, 105, 120, 133	95	1423	+ (0.47)	-
8.	31.09	*γ*-Elemene	204	Terpenoid	41, 55, 29, 93, 107, 119, 121	94	1437	+ (5.78)	-
9.	31.97	*α*-Humulene	204	Terpenoid	41, 51, 67, 80, 93, 105, 121	98	1458	+ (1.53)	-
10.	33.17	Germacrene D	204	Terpenoid	41, 67, 77, 81, 91, 105, 107	96,94	1485	+ (2.51)	+ (2.20)
11.	33.63	Docosane	310	Alkane	43, 57, 71, 85, 99	94	1496	-	+ (0.73)
12.	33.84	Curzerene	216	Terpenoid	41, 65, 108, 148, 216	93	1505	+ (21.55)	+ (2.39)
13.	36.47	Germacrene B	204	Terpenoid	41, 51, 53, 67, 93, 105, 121	94, 84	1565	+ (10.48)	+ (0.42)
14.	37.56	Viridiflorol	222	Terpenoid	41, 43, 55, 69, 71, 81, 105	87, 90	1592	+ (0.37)	-
15.	38.24	Curzerenone	230	Terpenoid	41, 65, 94, 107, 122	88	1609	+ (2.96)	-
16.	39.20	Isospathulenol	220	Terpenoid	43, 79, 91, 119, 147	88	1634	+ (1.12)	-
17.	41.65	*β*-Costol	220	Terpenoid	41, 67, 105, 121, 133	84	1696	+ (1.15)	-
18.	41.96	Germacrone	218	Terpenoid	41, 67, 79, 107, 121	92	1705	+ (5.91)	-
19.	42.17	*n*-Hentriacontane	436	Alkane	57, 71, 85, 99, 155	93	1710	-	+ (1.13)

20.	42.74	Androstan-17-one, 3-ethyl-3-hydroxy-, (5α)-	318	Steroid	79, 93, 135, 161	84	1726	+ (1.44)	-
21.	43.13	Curcumenol	234	Terpenoid	41, 65, 67, 91, 105, 119, 133	85	1736	+ (0.96)	-
22.	45.20	Cyclohexene, 4-pentyl-1-(4-propylcyclohexyl)-	276	Alkene	29, 41, 55, 67, 95, 109, 123	74	1792	+ (4.01)	-
23.	46.07	Hexadecanal	240	Alkane	29, 43, 68, 82, 96	89	1816	-	+ (0.44)
24.	47.07	Curcumenone	234	Terpenoid	43, 53, 65, 68, 79, 107, 123	95	1845	+ (1.50)	-
25.	47.32	(4S,5S)-Germacrone-4,5-epoxide	234	Terpenoid	41, 51, 53, 67, 68, 82, 105	83	1852	+ (2.24)	-
26.	47.82	Cembrene	272	Terpenoid	41,55, 81,93, 145,173	83	1864	+ (0.48)	-
27.	49.85	Tetracosane	338	Alkane	41, 43, 57, 71, 99, 127, 155	90	1925	-	+ (1.03)
28.	52.71	13-Octadecenal, (*Z*)-	266	Alkane	29, 41, 55, 69, 81, 111, 149	93	2009	-	+ (0.51)
29.	56.81	Dotriacontane	450	Alkane	29, 43, 57, 71, 99, 127, 155	85	2138	-	+ (0.73)
30.	63.92	(*E*)-Labda-8(17),12-diene-15,16-dial	302	Terpenoid	41, 69, 137, 147, 177	85	2380	+ (17.28)	-
31.	64.60	5-Hydroxy-7-methoxyflavanone	270	Flavonoid	39, 69, 95, 103, 138, 166, 193	92	2404	-	+ (0.79)
32.	67.45	2-Palmitoylglycerol	330	Alkane ester	29, 43, 69, 74, 98, 112, 147	89	2508	-	+ (1.28)
33.	69.96	5-Hydroxy-7-methoxyflavone	268	Flavonoid	39, 69, 95, 110, 137, 138	94	2604	-	+ (13.23)
34.	71.13	Unknown	298	Flavonoid	77, 105, 135, 171, 297	-	2650	-	+ (17.26)
35.	72.11	7,10-Octadecadienoic acid, methyl ester	294	Alkene ester	41, 67, 95, 109, 121, 150	87	2093	-	+ (1.77)
36.	74.86	5,7-Dimethoxyflavone	282	Flavonoid	39, 69, 90, 107, 122, 150	94	2801	-	+ (8.55)
37.	75.06	Decanedioic acid, bis(2-ethylhexyl) ester	426	Alkane ester	27, 41, 55, 57, 70, 84, 112	94	2809	-	+ (1.79)
38.	75.40	3,5,7-Trimethoxyflavone	312	Flavonoid	69, 77, 91, 105, 122, 142	85	2824	-	+ (5.19)
39.	78.39	5-Hydroxy-4',7-dimethoxyflavone	298	Flavonoid	39, 69, 95, 117, 135, 298	83	2952	-	+ (3.88)

40.	79.13	Unknown	328	Flavonoid	77, 135, 201, 242, 285, 328	-	2983	-	+ (10.32)
41.	82.71	3,4',5,7-Tetramethoxyflavone	342	Flavonoid	63, 77, 92, 119, 135, 342	75	3146	-	+ (3.77)
42.	83.06	5-Hydroxy-3,3',4',7-tetramethoxyflavone	358	Flavonoid	51, 79, 165, 315, 343, 358	81	3162	-	+ (1.98)
43.	85.74	Stigmasterol	412	Steroid	41, 55, 69, 91, 119, 133, 159	90	3279	-	+ (2.34)
44.	86.78	3,3',4',5,7-Pentamethoxyflavone	372	Flavonoid	63, 149, 172, 341, 357, 372	82	3324	-	+ (1.02)
45.	87.32	(3β)-stigmast-5-en-3-ol	414	Steroid	32, 41, 43, 81, 95, 121, 145	88	3345	+ (0.77)	+ (7.19)

Based on Table 2, 24 metabolites were identified in the KH hexane extract consisting of 21 terpenoids, 2 steroids, and 1 alkane. The metabolites presented in the highest concentrations (> 5.0% relative concentration) compared with the HH hexane extract were curzerene (21.55%), (*E*)-labda-8(17),12-diene-15,16-dial (17.28%), germacrene B (10.48%), and germacrone (5.91%), which could be proposed as chemical markers for KH. In a recent study by Mahanta et al. (2022) the GC-MS analysis of *C. caesia* essential oil harvested from a farm in Jorhat, India showed camphor, curzerenone, and 1,8-cineole as the major metabolites, each with concentrations of more than 10% [52]. The high concentration of curzerenone in the essential oil is due to curzerene being exposed to oxygen in the presence of light or heat leading to autoxidation. Most of the terpenoids detected in the current study were previously reported in the essential oil of KH collected from two provinces in India wherein camphor was detected as the major metabolite (17.82–25.16%) in KH from West Bengal province [53]. The extraction of the essential oil might have released more camphor vapour collected, condensed, and purified in the previous reported studies compared to the present study which used a normal hexane extraction method.

Meanwhile, twenty-seven metabolites were tentatively identified in the HH hexane extract of the rhizomes composed of flavonoids, alkanes, and terpenoids as the major metabolites. Based on Table 2, the major metabolites with more than 5% relative concentration were identified as 5-Hydroxy-7-methoxyflavone (13.23%), 5,7-Dimethoxyflavone (8.55%), (3*β*)-stigmast-5-en-3-ol (7.19%), and 3,5,7-Trimethoxyflavone (5.19%). Each of these metabolites was reported in the HH rhizome extract by GC-MS analysis in a previous study [30]. However, two unidentified metabolites appeared at 71.127 and 79.127 min with concentrations of 17.26% and 10.32%, respectively. However, further identification on these two constituents using PubChem database and compared with their molecular fragments has suggested them as 5-hydroxy-3,7-dimethoxyflavone and 5-hydroxy-3,7,4’-trimethoxyflavone respectively. Collectively, forty-five metabolites were tentatively identified, from both species covering terpenoids, flavonoids, steroids, and alkanes.

3.5. Complementary Relationship Between the NMR and GCMS Analyses

For comparison, the total metabolites detected through the NMR and GC-MS analyses of the two species are summarized in a Venn diagram (Fig. 8). For KH, 25 metabolites were detected through NMR and an additional 22 different metabolites were identified through the GCMS analysis, with two terpenoids detected in both platforms, namely camphor and germacrone affording the tentative identification of 47 metabolites. Meanwhile in the HH extract, 18 metabolites were detected through NMR and another 27 metabolites were identified in the GC-MS analysis, with three similar flavonoids detected in both platforms affording the identification of 42 metabolites. Most of the metabolites

identified in the NMR analysis ranged from polar to non-polar and encompassed amino acids, carbohydrates, terpenoids, and flavonoids (Table 1). Further identification using GC-MS on the hexane extract of the plant samples identified many more terpenoids in the KH extract and flavonoids in the HH extract.

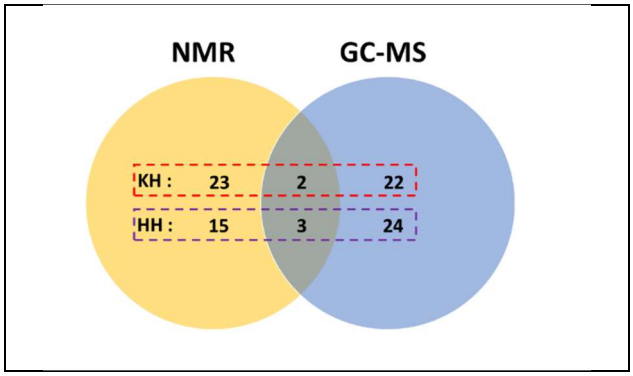

Figure 8. A Venn diagram showing the distribution of metabolites tentatively identified in the KH and HH rhizome extracts through NMR and GC-MS analyses

These findings demonstrate the advantage of NMR in recognizing distinct groups of substances through fingerprinting analysis. To compensate for the low sensitivity of NMR spectroscopy, the samples were submitted to GC-MS, a more sensitive analytical technique with detection levels varying from picomole to femtomole, allowing more secondary compounds to be explored [54–56]. However, due to its high sensitivity, MS is not a universal method that can identify a wide range of metabolite classes without secondary or tertiary ion analysis. The obtained data could be a complex forest of signals which is more complicated than NMR [57]. Therefore the combination of more than one analytical platform minimizes the shortcomings of using either NMR or MS alone and provides a broader metabolite profile.[58] Although there may be some initial ambiguity in identifying metabolites, hyphenation of the NMR and MS techniques will allow for the display of a wide variety of metabolites since both methods ultimately provide a more thorough identification with increased accuracy [58], [59].

In a recent study of metabolite fingerprinting among four Zingiberaceae spices, NMR was used as the main platform to differentiate their metabolite compositions into different chemical classes. In addition, GC-MS was used as a more sensitive analytical platform than NMR, leading to the discovery of 115 metabolites including sugars, diarylheptanoids, polyols, and organic, amino, and fatty acids [60]. In another study, thirty turmeric nutritional supplements were evaluated for their quality control using UHPLC-MS, and the results revealed a substantial diversity in their chemical composition, which was supported by ^{1}H-NMR spectroscopy and allowed for the absolute measurement of the primary bioactive compounds of curcuma [61]. Another example is of Tongkat Ali, also known as Malaysian Ginseng, where NMR metabolite fingerprinting discovered 15 main metabolites with the majority being sugars, organic acids, and fatty acids. Further analysis using solid-phase micro extraction (SPME)-GC-MS profiling revealed the presence of 59 volatiles, the majority of which were alcohols, aldehydes/furans, and sesquiterpene hydrocarbons [29].

4. Conclusions

This is the first study investigating the similarities and differences between the metabolite compositions of two species of the Zingiberaceae, *C. caesia* and *K. parviflora*, which may be mislabelled based on a similar local name, Kunyit Hitam (KH). The 1D- and 2D-NMR analyses successfully identified 25 metabolites in KH and 18 metabolites in HH comprised of amino acids, carbohydrates, terpenoids, and flavonoids. Several secondary metabolites are suggested as chemical markers for KH, including germacrone, zedoalactone A, zerumin B, and camphor, and four different methoxyflavones are suggested to characterize the HH extract. Further identification of the metabolites through GC-MS

disclosed 45 metabolites composed mainly of terpenoids, flavonoids, alkanes, steroids, and alkane esters. As summarized in a Venn diagram, 47 metabolites were identified in the KH extract, while 42 metabolites were identified in the HH extract, with only very few metabolites identified in both the NMR and GC-MS analyses. The combination of multi-platforms (NMR and GC-MS with MVDA) has proven to be a powerful tool for metabolite fingerprinting to address the authentication issues between these species which previously were solely based on morphology.

Acknowledgement

This study was partially supported by Berkat Curcuma Caesia Sdn. Bhd. and some assistance in terms of facilities by the Institute of Bioscience, Universiti Putra Malaysia.

Conflict of interest

All authors have declared no conflict of interest.

Supporting Information

Supporting information accompanies this paper on http://www.acgpubs.org/journal/records-of-natural-products

ORCID
Muhammad Safwan Ahamad Bustamam: 0000-0002-5357-4070
Siok-Geok Chong: 0000-0002-8337-6841
Wei-Meng Heng: 0009-0005-5133-2560
M. Akmal M. Nazri: 0009-0008-1329-3224
Emelia Asmara Md Daud: 0009-0001-0716-2171
Nur Aqilah Lakowi: 0009-0009-2588-7000
Mohd Saipullah Mohd Daud: 0009-0008-6799-1191
Geoffrey A. Cordell: 0000-0003-2536-3097
Intan Safinar Ismail: 0000-0003-3960-0022

References

[1] P. Paliwal, S. S. Pancholi and R. K. Patel (2011). Pharmacognostic parameters for evaluation of the rhizomes of *Curcuma caesia*, *J. Adv. Pharm. Technol. Res.* **2**, 56–61.

[2] N. N. A. Ibrahim, W. A. Wan Mustapha, N. S. Sofian-Seng, S. J. Lim, N. S. Mohd Razali, A. H. Teh, H. A. Rahman and A. Mediani (2023). A Comprehensive review with future prospects on the medicinal properties and biological activities of *Curcuma caesia* roxb., *Evidence-based Complement. Altern. Med.* **1**, 7006565.

[3] Y. Liu, S. S. Roy, R. H. C. Nebie, Y. Zhang and M. G. Nair (2013). Functional food quality of *Curcuma caesia*, *Curcuma zedoaria* and *Curcuma aeruginosa* endemic to Northeastern India, *Plant Foods Hum. Nutr.* **68**, 72–77.

[4] A. Borah, M. Paw, R. Gogoi, R. Loying, N. Sarma, S. Munda, S. K. Pandey and M. Lal (2019). Chemical composition, antioxidant, anti-inflammatory, anti-microbial and in-vitro cytotoxic efficacy of essential oil of *Curcuma caesia* Roxb. leaves: An endangered medicinal plant of North East India, *Ind. Crops Prod.* **129**, 448–454.

[5] D. Pandey and A. K. Gupta (2014). Antibacterial efcacy of *Curcuma caesia* from bastar district of Chhattisgarh, India, *Int. J. Pharm. Sci. Res.* **5**, 2294–2301.

[6] A. Jain and D. K. Parihar (2018). In-vitro antidiabetic potential of endangered *Curcuma caesia* rhizome extracts and its characterization by FTIR and GC/HR-MS analysis, *Int. J. Adv. Sci. Eng. Technol.* **6**, 16–22.

[7] P. Majumder, S. Mazumder, M. Chakraborty, S. G. Chowdhury, S. Karmakar and P. K. Haldar (2017). Preclinical evaluation of Kali Haldi (*Curcuma caesia*): A promising herb to treat type-2 diabetes, *Orient.*

Pharm. Exp. Med. **17**, 161–169.

[8] S. B. Sawant, G. Bihani, S. Mohod and S. Bodhankar (2014). Evaluation of analgesic and anti-infammatory activity of methanolic extract of *Curcuma caesia* Roxb. rhizomes in laboratory animals, *Int. J. Pharm. Pharm. Sci.* **6**, 243–247.

[9] S. V. Bharathi, V. Anuradha, A. L. I. Ahmad and S. M. Tajo (2017). Trombolytic activity of *Curcuma amada* and *Curcuma caesia*, *Asian J. Pharm. Clin. Res.* **10**, 317–318.

[10] G. R. Angel, B. Vimala, and B. Nambisan (2013). Antioxidant and anti-infammatory activities of proteins isolated from eight Curcuma species, *Phytopharmacology* **4**, 96–105.

[11] I. Karmakar, P. Saha, N. Sarkar, S. Bhattacharya and P. K. Haldar (2011). Neuropharmacological assessment of *Curcuma caesia* rhizome in experimental animal models, *Orient. Pharm. Exp. Med.* **11**, 251–255.

[12] L. Kma, R. N. Sharan and K. L. Hadem (2014). Inhibitory potential of methanolic extracts of *Aristolochia tagala* and *Curcuma caesia* on hepatocellular carcinoma induced by diethylni- trosamine in BALB/c mice, *J. Carcinog.* **13**, 7–10.

[13] S. Saokaew, P. Wilairat, P. Raktanyakan, P. Dilokthornsakul, T. Dhippayom, C. Kongkaew, R. Sruamsiri, A. Chuthaputti and N. Chaiyakunapruk (2017). Clinical Effects of Krachaidum (*Kaempferia parviflora*): A Systematic Review, *J. Evidence-Based Complement. Altern. Med.* **22**, 413–428.

[14] J. Yu, X. Wu, C. Liu, S. Newmaster, S. Ragupathy and W. J. Kress (2021). Progress in the use of DNA barcodes in the identification and classification of medicinal plants, *Ecotoxicol. Environ. Saf.* **208**, 111691.

[15] WHO (2018). Annex 1: WHO guidelines on good herbal processing practices for herbal medicines, WHO Technical Report Series, No. 1010. 81–152, [Online]. Available: https://apps.who.intmedicinedocs/documents/s23449en/s23449en.pdf

[16] Y. Liang, P. Xie and K. Chan (2004). Quality control of herbal medicines, *J. Chromatogr. B* **812**, 53–70.

[17] P. Wang and Z. Yu (2015). Species authentication and geographical origin discrimination of herbal medicines by near infrared spectroscopy: A review, *J. Pharm. Anal.* **5**, 277–284.

[18] D. Guo (2017). Quality marker concept inspires the quality research of traditional chinese medicines, *Chinese Herb. Med.* **9**, 1–2.

[19] A. Rohman, E. A. Rawar, S. Sudevi, A. F. Nurrulhidayah and A. Windarsih (2020). The use of chemometrics in combination with molecular spectroscopic and chromatographic methods for authentication of Curcuma species: A review, *Food Res. Int.* **4**, 1850–1858.

[20] C. Toniolo, M. Nicoletti, F. Maggi and A. Venditti (2014). HPTLC determination of chemical composition variability in raw materials used in botanicals, *Nat. Prod. Res.* **28**, 119–126.

[21] M. Syed, M. N. Khan, A. Khadim, H. Shadab, A. Perveen, H. R. El-Seedi and S. G. Musharraf (2021). Chemical fingerprinting of three Anemone species and an adulteration study to detect cross mixing of medicinal plants by HPLC-HR-ESI-MS/MS method, *J. King Saud Univ. - Sci.* **33**, 101461.

[22] F. D. O. Riswanto, A. Windarsih, E. Lukitaningsih, M. Rafi, N. A. Fadzilah and A. Rohman (2022). Metabolite fingerprinting based on ^{1}H-NMR spectroscopy and liquid chromatography for the authentication of herbal products, *Molecules* **27**, 1–17.

[23] C. Deborde, J.-X. Fontaine, D. Jacob, A. Botana, V. Nicaise, F. Richard-Forget, S. Lecomte, C. Decourtil, K. Hamade and F. Mesnard (2019). Optimizing 1D ^{1}H-NMR profiling of plant samples for high throughput analysis: Extract preparation, standardization, automation and spectra processing, *Metabolomics* **15**, 28.

[24] M. S. Gholkar, J. V. Li, P. G. Daswani, P. Tetali and T. J. Birdi (2021). ^{1}H Nuclear magnetic resonance-based metabolite profiling of guava leaf extract: An attempt to develop a prototype for standardization of plant extracts, *BMC Complement. Med. Ther.* **21**, 95.

[25] P. H. Hatumura, G. S. de Oliveira, G. G. Marcheafave, M. Rakocevic, R. E. Bruns, I. S. Scarminio and A. E. Terrile (2018). Chemometric analysis of ^{1}H-NMR fingerprints of coffea arabica green bean extracts cultivated under different planting densities, *Food Anal. Methods* **11**, 1906–1914.

[26] E. Belmonte-Sánchez, R. Romero-González, and A. Garrido Frenich (2021). Applicability of high-resolution NMR in combination with chemometrics for the compositional analysis and quality control of spices and plant-derived condiments, *J. Sci. Food Agric.* **101**, 3541–3550.

[27] L. H. Nurani, A. Rohman, A. Windarsih, A. Guntarti, F. D. O. Riswanto, E. Lukitaningsih, N. A. Fadzillah, and *et al.* (2021). Metabolite fingerprinting using ^{1}H-NMR spectroscopy and chemometrics for classification of three curcuma species from different origins, *Molecules* **26**, 1–13.

[28] A. Rivera-Pérez, R. Romero-González and A. Garrido Frenich (2022). A metabolomics approach based on 1H NMR fingerprinting and chemometrics for quality control and geographical discrimination of black pepper, *J. Food Compos. Anal.* **105**, 104235.

[29] A. Serag, A. Zayed, A. Mediani and M. A. Farag (2023). Integrated comparative metabolite profiling via NMR and GC–MS analyses for tongkat ali (*Eurycoma longifolia*) fingerprinting and quality control analysis, *Sci. Rep.* **13**, 1–15.

[30] R. S. Atom, S. A. M. Shaikh, K. Maharabam, R. Khunjamayum, D. Ahanthem, W. S. Laitonjam, R. S. Ningthoujam and A. Kunwar (2022). GC-MS profiling, in vitro antioxidant and antimicrobial activities of *Kaempferia parviflora* Wall. ex. Baker rhizome extract, *Int. J. Pharm. Investig.* **12**, 430–437.

[31] D. K. Poudel, P. K. Ojha, A. Rokaya, R. Satyal, P. Satyal and W. N. Setzer (2022). Analysis of volatile constituents in curcuma species, viz. *C. aeruginosa*, *C. zedoaria*, and *C. longa*, from Nepal, *Plants* **11**, 1–12.

[32] S. Y. Wang, H. Zhao, H. T. Xu, X. D. Han, Y. S. Wu, F. F. Xu, X. B. Yang, U. Göransson and B. Liu (2021). *Kaempferia galanga* L.: Progresses in phytochemistry, pharmacology, toxicology and ethnomedicinal uses, *Front. Pharmacol.* **12**, 1–17.

[33] S. L. Lee, C. T. Lee, L. H. Tnah, Z. Nurul Farhanah, K. K. S. Ng and C. H. Ng (2015). FRIM's standard operating procedure on forensic dna testing for plant species identification and timber tracking, version 1.1.

[34] N. Komonsing, P. Khuwijitjaru, M. Nagle, J. Müller and B. Mahayothee (2022). Effect of drying temperature together with light on drying characteristics and bioactive compounds in turmeric slice, *J. Food Eng.* **317**, 110695.

[35] L. Eriksson, E. Johansson, N. Kettaneh-Wold, J. Trygg, C. Wikstrom and S. Wold (2006). Multi- and megavariate data analysis part 1: Basic principles and applications. Umeå, Sweden: Umetrics Academy.

[36] S. S. Baghel, R. S. Baghel, K. Sharma, and I. Sikarwar (2013). Pharmacological activities of *Curcuma caesia*, *Int. J. Green Pharm.* **7**, 1–5.

[37] C. D. Labrooy, T. L. Abdullah, and J. Stanslas (2018). Identification of ethnomedicinally important Kaempferia L. (Zingiberaceae) species based on morphological traits and suitable DNA region, *Curr. Plant Biol.* **14**, 50–55.

[38] N. N. A. Ibrahim, N. Kamal, A. Mediani, A. A. B. Sajak, S. Y. Lee, K. Shaari, and H. A. Rahman (2023). ^{1}H-NMR-based metabolomics approach revealing metabolite variation of black turmeric (*Curcuma caesia*) extracts and correlation with its antioxidant and α-glucosidase inhibitory activities, *Food Technol. Biotechnol.* **61**, 104–117.

[39] R. Maurya, P. Gupta, C. S. Chanotiya, S. S. Dhawan, S. Srivastava, A. Yadav, A. Kumar, Y. Swamy and R.K. Lal (2022). Investigation of monoterpenoids rich essential oils of two *Ocimum basilicum* L. varieties at different agro-climatic conditions in India, *Acta Ecol. Sin.* **42**, 1–10.

[40] R. S. Policegoudra, K. Abiraj, D. C. Gowda and S. M. Aradhya (2007). Isolation and characterization of antioxidant and antibacterial compound from mango ginger (*Curcuma amada* Roxb.) rhizome, *J. Chromatogr. B Anal. Technol. Biomed. Life Sci.* **852**, 40–48.

[41] T. Awin, A. Mediani, Maulidiani, S. W. Leong, S. M. Muhd Faudzi, K. Shaari, and F. Abas (2019). Phytochemical and bioactivity alterations of Curcuma species harvested at different growth stages by NMR-based metabolomics, *J. Food Compos. Anal.* **77**, 66–76.

[42] Y. Jung, J. Lee, H. K. Kim, B. C. Moon, Y. Ji, D. H. Ryu and G. S. Hwang (2012). Metabolite profiling of Curcuma species grown in different regions using ^{1}H-NMR spectroscopy and multivariate analysis, *Analyst* **137**, 5597–5606.

[43] K. Sutthanut, B. Sripanidkulchai, C. Yenjai and M. Jay (2007). Simultaneous identification and quantitation of 11 flavonoid constituents in *Kaempferia parviflora* by gas chromatography, *J. Chromatogr. A* **1143**, 227–233.

[44] I. Mendoza-Poudereux, E. Kutzner, C. Huber, J. Segura, I. Arrillaga and W. Eisenreich (2017). Dynamics of monoterpene formation in spike lavender plants, *Metabolites* **7**,65.

[45] F. Abas, N. H. Lajis, K. Shaari, D. A. Israf, J. Stanslas, U. K. Yusuf and S. M. Raof (2005). A labdane diterpene glucoside from the rhizomes of *Curcuma mangga*, *J. Nat. Prod.* **68**, 1090–1093.

[46] L. T. Loan, P. Thi, A. Hue and M. C. Thanh (2023). Flavonoids from the Rhizomes of *Kaempferia Parviflora* Wall . Ex Baker, *J. Sci.* **39**, 100–107.

[47] C. Chen, K. W. Krausz, Y. M. Shah, J. R. Idle§ and F. J. Gonzalez (2009). Serum metabolomics reveals irreversible inhibition of fatty acid β-oxidation through the suppression of pparα activation as a contributing mechanism of acetaminophen-induced hepatotoxicity, *Chem. Res. Toxicol.* **22**, 699–707.

[48] L. Eriksson, J. Trygg and S. Wold (2008). CV-ANOVA for significance testing of PLS and ® OPLS models, *J. Chemom.* **22**, 594–600.

[49] H. M. Woo, K. M. Kim, M. H. Choi, B. H. Jung, J. Lee, B. C. Kong, G. Nam, S.J. Kim, S. Bai and S.W. Chung (2009). Mass spectrometry based metabolomic approaches in urinary biomarker study of women's cancers, *Clin. Chim. Acta* **400**, 63–69.

[50] S. Rajkumari and K. Sanatombi (2018). Nutritional value, phytochemical composition, and biological activities of edible Curcuma species: A review, *Int. J. Food Prop.* **20**, S2668–S2687.

[51] A. Singh, N. Singh, S. Singh, R. P. Srivastava, L. Singh, P. C. Verma, H. P. Devkota, L. Rahman, B. K. Rajak, A. Singh and *et al.* (2023). The industrially important genus Kaempferia: An ethnopharmacological review, *Front. Pharmacol.* **14**, 1–18.

[52] B. P. Mahanta, P. Kemprai, P. K. Bora, M. Lal, and S. Haldar (2022). Phytotoxic essential oil from black turmeric (*Curcuma caesia* Roxb.) rhizome: Screening, efficacy, chemical basis, uptake and mode of transport, *Ind. Crops Prod.* **180**, 114788.

[53] S. Singh, B. C. Sahoo, A. Ray, S. Jena, M. Dash, S. Nayak, B. Kar and S. Sahoo (2021). Intraspecific chemical variability of essential oil of *Curcuma caesia* (Black Turmeric), *Arab. J. Sci. Eng.*, **46**, 191–198.

[54] L. W. Sumner, P. Mendes and R. A. Dixon (2003). Plant metabolomics: Large-scale phytochemistry in the functional genomics era, *Phytochemistry* **62**, 817–836.

[55] M. Bedair and L. Sumner (2008). Current and emerging mass-spectrometry technologies for metabolomics, *Trends Anal. Chem.* **27**, 238–250.

[56] D. A. Skoog, D. M. West, F. J. Holler, and S. R. Crouch (2014). Fundamentals of Analytical Chemistry, 9th Edition.

[57] A.-H. M. Emwas, R. M. Salek, J. L. Griffin and J. Merzaban (2013). NMR-based metabolomics in human disease diagnosis : Applications , limitations , and recommendations, *Metabolomics*, **9**, 1048–1072.

[58] D. D. Marshall and R. Powers (2017). Beyond the paradigm : Combining mass spectrometry and nuclear magnetic resonance for metabolomics, *Prog. Nucl. Magn. Reson. Spectrosc.* **100**, 1–16.

[59] D. Marshall, S. Lei, B. Worley, Y. Huang, A. Garcia-Garcia, R. Franco, E. Dodds and R. Powers (2015). Combining DI-ESI-MS and NMR datasets for metabolic profiling, *Metabolomics* **11**, 391– 402.

[60] A. R. Khattab, D. M. Rasheed, A. E. El-Haddad, A. Porzel, L. A. Wessjohann and M. A. Farag (2022). Assessing phytoequivalency of four Zingiberaceae spices (galangals, turmeric and ginger) using a biochemometric approach: A case study, *Ind. Crops Prod.* **188**, 115722.

[61] S. Sorng, S. Balayssac, S. Danoun, G. Assemat, A. Mirre, V. Cristofoli, A. C. Le Lamer, V. Jullian, V. Gilard and N. Fabre (2022). Quality assessment of Curcuma dietary supplements: Complementary data from LC-MS and ^{1}H-NMR, *J. Pharm. Biomed. Anal.* **212**, 114631.